Cao, X., Ni, B., Summers, D., Shprits, Y., Gu, X., Fu, S., Lou, Y., Zhang, Y., Ma, X., Zhang, W., Huang, H., Yi, J. (2019): Sensitivity of EMIC Wave-Driven Scattering Loss of Ring Current Protons to Wave Normal Angle Distribution. - *Geophysical Research Letters*, *46*, 2, pp. 590—598.

DOI: http://doi.org/10.1029/2018GL081550

Geophysical Research Letters

RESEARCH LETTER
10.1029/2018GL081550

Key Points:
- The wave normal angle distribution strongly affects the EMIC wave-driven scattering loss of ring current protons
- Quantitative differences in the diffusion coefficients between field-aligned and oblique waves are presented
- Pitch-angle scattering of higher-energy ring current protons is more sensitive to the variation of wave normal angle distribution

Correspondence to:
B. Ni,
bbni@whu.edu.cn

Citation:
Cao, X., Ni, B., Summers, D., Shprits, Y. Y., Gu, X., Fu, S., et al. (2019). Sensitivity of EMIC wave-driven scattering loss of ring current protons to wave normal angle distribution. *Geophysical Research Letters*, *46*, 590–598. https://doi.org/10.1029/2018GL081550

Received 3 DEC 2018
Accepted 7 JAN 2019
Accepted article online 11 JAN 2019
Published online 24 JAN 2019

Sensitivity of EMIC Wave-Driven Scattering Loss of Ring Current Protons to Wave Normal Angle Distribution

Xing Cao[1], Binbin Ni[1], Danny Summers[2], Yuri Y. Shprits[3,4,5], Xudong Gu[1], Song Fu[1], Yuequn Lou[1], Yang Zhang[1], Xin Ma[1], Wenxun Zhang[1], He Huang[1], and Juan Yi[1]

[1]Department of Space Physics, School of Electronic Information, Wuhan University, Wuhan, China, [2]Department of Mathematics and Statistics, Memorial University of Newfoundland, St. Johns, Newfoundland, Canada, [3]Helmholtz Centre Potsdam, GFZ German Research Centre for Geosciences, Potsdam, Germany, [4]Institute of Physics and Astronomy, University of Potsdam, Potsdam, Germany, [5]Department of Earth, Planetary, and Space Sciences, University of California, Los Angeles, California, USA

Abstract Electromagnetic ion cyclotron waves have long been recognized to play a crucial role in the dynamic loss of ring current protons. While the field-aligned propagation approximation of electromagnetic ion cyclotron waves was widely used to quantify the scattering loss of ring current protons, in this study, we find that the wave normal distribution strongly affects the pitch angle scattering efficiency of protons. Increase of peak normal angle or angular width can considerably reduce the scattering rates of ≤10 keV protons. For >10 keV protons, the field-aligned propagation approximation results in a pronounced underestimate of the scattering of intermediate equatorial pitch angle protons and overestimates the scattering of high equatorial pitch angle protons by orders of magnitude. Our results suggest that the wave normal distribution of electromagnetic ion cyclotron waves plays an important role in the pitch angle evolution and scattering loss of ring current protons and should be incorporated in future global modeling of ring current dynamics.

Plain Language Summary Electromagnetic ion cyclotron (EMIC) wave is a class of electromagnetic wave that is frequently observed in the Earths' magnetosphere. EMIC waves can cause the loss of ring current protons by scattering them into the atmosphere. Previous attempts to quantify the loss of ring current protons by EMIC waves are mostly limited to the assumption that the waves are propagating exactly along the direction of geomagnetic field line. In this study, we show that this assumption will seriously break down once the waves are obliquely propagating. The obliquity of EMIC waves not only influences the pitch angle evolution of ring current protons but also affects their loss time scales. Our study confirms the importance of including the obliquity of EMIC waves in the modeling efforts of ring current dynamics.

1. Introduction

As a commonly observed wave mode in the Earth's magnetosphere, electromagnetic ion cyclotron (EMIC) waves are excited by a temperature anisotropy of 1–100 keV ions (Anderson et al., 1996; Chen et al., 2010; Cornwall, 1965; Wang et al., 2016; Zhang et al., 2014) and propagate in three distinct frequency bands (H^+, He^+, and O^+) separated by the corresponding ion gyrofrequencies. EMIC waves have long been recognized to account for the efficient precipitation loss of outer belt relativistic electrons (e.g., Cao, Ni, et al., 2017; Cao, Yuri, et al., 2017; Kersten et al., 2014; Liu et al., 2010; Meredith et al., 2003; Miyoshi et al., 2008; Ni et al., 2015; Rodger et al., 2008; Shprits et al., 2016, 2017; Summers & Thorne, 2003; Usanova et al., 2014; Zhang et al., 2016), while the resonant interactions between EMIC waves and protons can take place over a very broad spatial range in the magnetosphere. Xiao et al. (2013) proposed that EMIC waves in the magnetospheric cusp can efficiently scatter protons into the atmosphere and produce the cusp proton aurora. Pitch angle scattering by EMIC waves has been proposed as one of the dominant mechanisms responsible for the rapid decay of the terrestrial ring current during geomagnetic storms (e.g., Daglis et al., 1999; Erlandson & Ukhorskiy, 2001; Jordanova et al., 1997; Kozyra et al., 2013; Summers, 2005; Usanova et al., 2010; Yahnin & Yahnina, 2007) and the evolution of the partial ring current ion pitch angle distributions (Runov et al., 2016). The subsequent proton precipitation losses have been confirmed by previous observations (Fuselier et al., 2004; Sakaguchi et al., 2007; Spasojevic et al., 2011; Su et al., 2011) to account for the formation of detached proton arcs at subauroral latitudes. Recently, it was suggested by Liang et al. (2014) and Cao et al. (2016) that EMIC waves could be a potential candidate for the "reversed" energy-latitude precipitation pattern of central plasma sheet protons.

The Earth's ring current consists of energetic ions coming from both the ionosphere and solar wind, the major carriers being protons with energies from 1 keV to a few hundred keV (Daglis et al., 1999; Gkioulidou et al., 2016; Zhao et al., 2015). Pitch angle scattering by EMIC waves has been incorporated into global ring current modeling (Gamayunov et al., 2009; Jordanova et al., 2001; Khazanov et al., 2006; Kozyra et al., 2013) to account for the rapid decay of ring current protons. While most previous attempts to quantify the scattering loss of ring current protons are limited to the assumption that EMIC waves are parallel propagating (e.g., Erlandson & Ukhorskiy, 2001; Summers, 2005; Xiao et al., 2011, 2012), recent statistical studies of EMIC wave global distribution have demonstrated the high occurrence rates of EMIC wave events with large wave normal angle (Allen et al., 2015; Min et al., 2012; Saikin et al., 2015). It is well recognized that the wave normal distribution plays an important role in the resonant interactions between radiation belt electrons and various magnetospheric waves including plasmaspheric hiss, chorus, and magnetosonic waves (Albert, 2017; Artemyev et al., 2012; Gao et al., 2015; Lei et al., 2017; Li et al., 2014; Meredith et al., 2007; Mourenas et al., 2012; Shprits, Thorne, et al., 2006; Shprits & Ni, 2009). However, to the best of our knowledge, there has been little research aimed at understanding how the wave normal angle distribution affects the scattering loss of ring current protons by EMIC waves. This is the focus of the present study.

2. Model Description

Along with previous studies (e.g., Glauert & Horne, 2005; He et al., 2016; Kersten et al., 2014; Li et al., 2007; Ni et al., 2015; Summers et al., 2007a), we assume the EMIC wave spectral intensity I_B has a Gaussian distribution given by

$$I_B(\omega) = \mathrm{A}\exp\left[-\left(\frac{\omega-\omega_m}{\delta\omega}\right)^2\right](\omega_{lc}\leq\omega\leq\omega_{uc}), \tag{1}$$

where ω_{lc} and ω_{uc} are the lower and upper cutoff frequencies, ω_m and $\delta\omega$ are the peak wave frequency and spectral bandwidth, and A is a normalization constant given by

$$A = \frac{B_w^2}{\delta\omega}\frac{2}{\pi^{1/2}}\left[\mathrm{erf}\left(\frac{\omega_m-\omega_{lc}}{\delta\omega}\right) + \mathrm{erf}\left(\frac{\omega_{uc}-\omega_m}{\delta\omega}\right)\right]^{-1}, \tag{2}$$

where B_w is the wave amplitude and erf is the error function. The normal angle distribution of EMIC waves is also assumed to be Gaussian, given by

$$g(\theta) = \exp\left[-\left(\frac{\tan\theta-\tan\theta_m}{\tan\theta_w}\right)^2\right](\theta_{lc}\leq\theta\leq\theta_{uc}), \tag{3}$$

where θ is the wave normal angle, θ_{w} is the angular width, θ_m is the normal angle with peak wave power, and θ_{lc} and θ_{uc} are the lower and upper bounds to the wave normal angle distribution.

The Doppler-shifted gyroresonance condition between electromagnetic waves and protons is given by the equation (e.g., Summers, 2005)

$$\omega-k_\parallel v_\parallel = N\Omega_p/\gamma \tag{4}$$

where ω is the wave frequency, $k_\parallel = k\cos\theta$ is the parallel component of wave number k, $v_\parallel = v\cos\alpha$ is the parallel component of proton velocity v, Ω_p is the proton gyrofrequency, $\gamma = (1-v^2/c^2)^{-1/2}$ is the Lorentz factor, N is the resonance order, and c is the speed of light. Equation (4) corresponds to the Landau resonance condition when $N = 0$ and corresponds to the cyclotron resonance condition when $N = \pm1, \pm2, \pm3, \ldots$. Note that for parallel propagating EMIC waves (i.e., $\theta = 0^\circ$), only the primary cyclotron resonance order $N = 1$ contributes to resonant scattering of protons (Summers, 2005).

To evaluate the scattering loss of ring current protons by resonant interactions with EMIC waves, we use the Full Diffusion Code (Cao et al., 2016; Cao, Ni, et al., 2017; Ni et al., 2008, 2015, 2018; Shprits & Ni, 2009) to

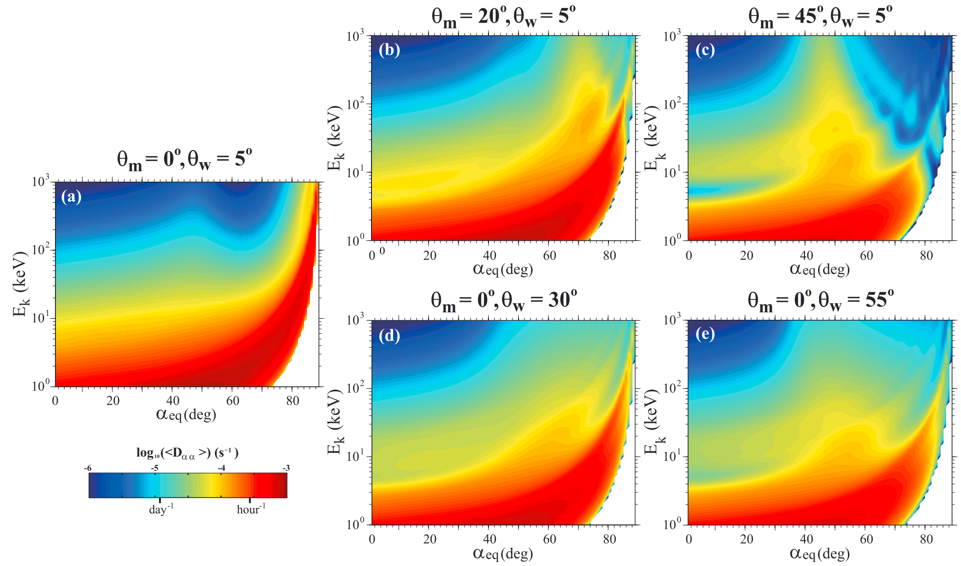

Figure 1. The 2-D plots of bounce-averaged pitch-angle diffusion coefficients $<D_{\alpha\alpha}>$ due to EMIC waves as a function of proton kinetic energy E_k and equatorial pitch angle $\alpha_{\rm eq}$ for indicated sets of peak wave normal angle θ_m and angular width θ_w.

calculate the quasi-linear bounce-averaged pitch angle diffusion coefficients by obliquely propagating EMIC waves in a multiion (H^+, He^+, and O^+) plasma. In the present study, we adopt a nominal wave amplitude of 1 nT and the results for arbitrary wave amplitude can be easily obtained, since diffusion coefficients are proportional to the square of wave amplitude in the quasi-linear regime (Albert, 2007; Summers et al., 2007b). We focus on the L-shell $L = 6$ and adopt a typical frequency spectrum of H^+ band EMIC waves used in previous studies (Ni et al., 2015; Summers et al., 2007a; Summers & Thorne, 2003), that is, $\omega_{lc} = 0.5\Omega_p$, $\omega_{uc} = 0.7\Omega_p$, $\omega_m = 0.6\Omega_p$, and $\delta\omega = 0.1\Omega_p$. We set the ion concentration ratios as $\eta_{H^+} = 0.85$, $\eta_{He^+} = 0.1$, and $\eta_{O^+} = 0.05$, where $\eta_{H^+} = N_{H^+}/N_e$; $\eta_{He^+} = N_{He^+}/N_e$; $\eta_{O^+} = N_{O^+}/N_e$; and N_e, N_{H^+}, N_{He^+}, and N_{O^+} denote the ambient electron (e^-), hydrogen (H^+), helium (He^+), and oxygen (O^+) ion number density, respectively. The electron number density N_e is adopted from the plasmaspheric density model of Sheeley et al. (2001). In our calculations, we choose the L-mode branch of cold plasma dispersion relation and neglect the coupling of pure L-mode to R-mode or mixed polarization, following the study of Albert (2003). There are two criteria for the determination of the maximum latitude of wave confinement. The first one is 40°, which is assumed based on previous statistical observations (e.g., Allen et al., 2015). The second one is the latitude where the waves reaches the stopband and cannot propagate to higher latitudes. Then we choose the small value of these two latitudes as the maximum latitude of wave confinement. As in previous studies (Cao et al., 2016; He et al., 2016; Ni et al., 2015), we assume that the ambient electron density remains constant along the field line. Our calculations of EMIC wave-induced quasi-linear scattering rates of ring current protons include contributions from the $N = -20$ to 20 cyclotron harmonic resonances and the Landau resonance ($N = 0$).

3. Numerical Results

Based on previous statistical observations of the EMIC wave normal angle (Allen et al., 2015; Saikin et al., 2015), we choose a fixed set of lower and upper bounds of normal angle, that is, $\theta_{\rm lc} = 0°$ and $\theta_{\rm uc} = 60°$. In order to investigate the influence of wave normal angle on the EMIC wave-driven loss of ring current protons, we consider three sets of peak wave normal angle θ_m and three sets of angular width $\theta_{\rm w}$. In Figures 1a–1c, we present the bounce-averaged pitch angle diffusion coefficients $<D_{\alpha\alpha}>$ as a function of proton kinetic energy E_k and equatorial pitch angle $\alpha_{\rm eq}$ for $\theta_{\rm m} = 0°$ (field-aligned), 20° (oblique), and 45° (highly oblique), respectively, while $\theta_{\rm w} = 5°$ is kept constant. It is shown that the resonant interactions between EMIC waves and ring current protons occur over a very broad pitch angle and energy coverage and the

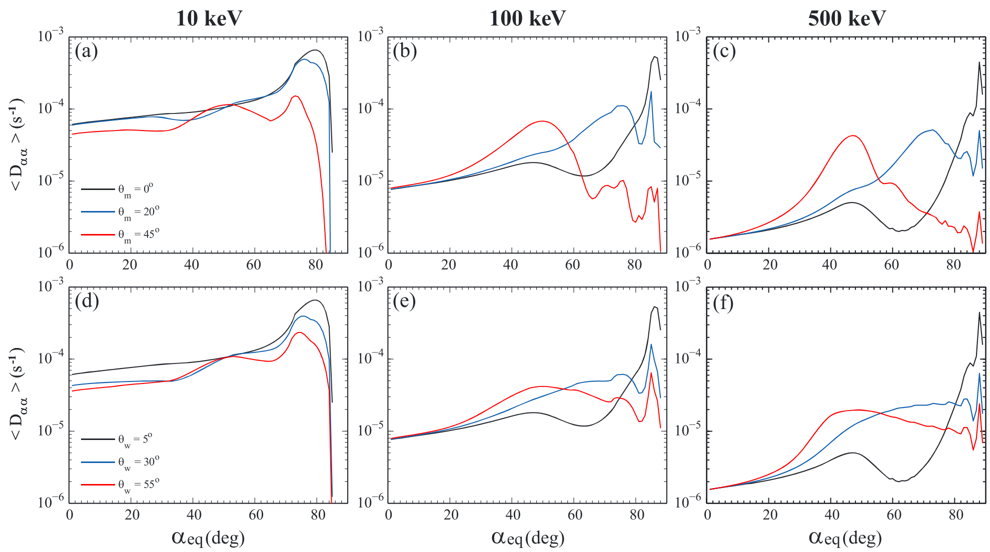

Figure 2. Line plots of bounce-averaged pitch angle diffusion coefficients $<D_{\alpha\alpha}>$ due to EMIC waves as a function of equatorial pitch angle α_{eq} for the indicated proton energies. (a–c) The results for different peak wave normal angles θ_m and a fixed angular width $\theta_w = 5°$. (d–f) The results for different angular widths θ_w and a fixed peak normal angle $\theta_m = 0°$.

corresponding resonant region tends to extend to larger pitch angle as the proton energy increases, regardless of the wave normal angle distribution. The time scales associated with the scattering of ring current protons range from tens of minutes to several days. For field-aligned waves, the strongest pitch angle diffusion is found at 1–10 keV on a time scale of <1 hr, and shifts to larger pitch angles as proton energy increases. Figures 1a–1c show that the sensitivity of pitch angle scattering rates to the variation of peak wave normal angle θ_m is strongly dependent on proton energy. For ≤10 keV protons, the scattering efficiency decreases as the wave normal becomes more and more oblique. For >10 keV protons, an increase of peak wave normal angle θ_m does not significantly change the pitch angle scattering rates at low α_{eq} but causes pronounced modification of scattering rates for $\alpha_{eq} > 30°$. As θ_m increases to 20°, we can clearly see the increase of scattering rates for α_{eq}~50° to 80° and the decrease of scattering rates for $\alpha_{eq} > 80°$. For highly oblique waves (i.e., $\theta_m = 45°$), the pitch angle scattering efficiency of >10 keV protons peaks at α_{eq} = ~40°–65° and is found to be much weaker than field-aligned waves for $\alpha_{eq} > 65°$. Especially for near-equatorially mirroring protons ($\alpha_{eq} > 80°$), the decrease of scattering rates can be even larger than 2 orders of magnitude.

We now investigate the sensitivity of proton bounce-averaged pitch angle scattering rates to the variation of angular width θ_w in Figures 1a, 1d, and 1e, which correspond to three different wave normal angle models: $\theta_w = 5°$ (field-aligned), 30° (narrow), and 55° (wide), respectively. For these three cases, the peak of wave normal angle is assumed to be along the ambient magnetic field line. Similar to the variation of θ_w, a widening of the wave normal distribution will cause a decrease of the scattering rates of ≤10 keV protons. Pronounced changes of scattering rates are mainly found in the resonant interactions between EMIC waves and >10 keV protons. For these protons, scattering rates increase at intermediate α_{eq} and decrease at α_{eq} close to 90°, and such changes in scattering rates become more obvious as the angular width increases. Figure 1 also shows that the pitch angle scattering of ring current protons due to EMIC waves is more sensitive to the variation of peak wave normal angle than that of angular width.

In Figure 2, we illustrate the line plots of proton bounce-averaged pitch angle diffusion coefficients $<D_{\alpha\alpha}>$ due to EMIC waves as a function of equatorial pitch angle α_{eq} for 10, 100, and 500 keV protons. Figures 2a–2c show the results for different peak wave normal angle θ_m and a fixed angular width $\theta_w = 5°$, while Figures 2d and 2e show the results for different angular width θ_w and a fixed peak normal angle $\theta_m = 0°$. Figure 2 clearly shows that pitch angle scattering of higher-energy protons is more sensitive to the variation of wave normal angle distribution than that of lower energy protons. For 10 keV protons, the increase of θ_m and θ_w will result in the decrease of scattering rates and the most pronounced decrease is

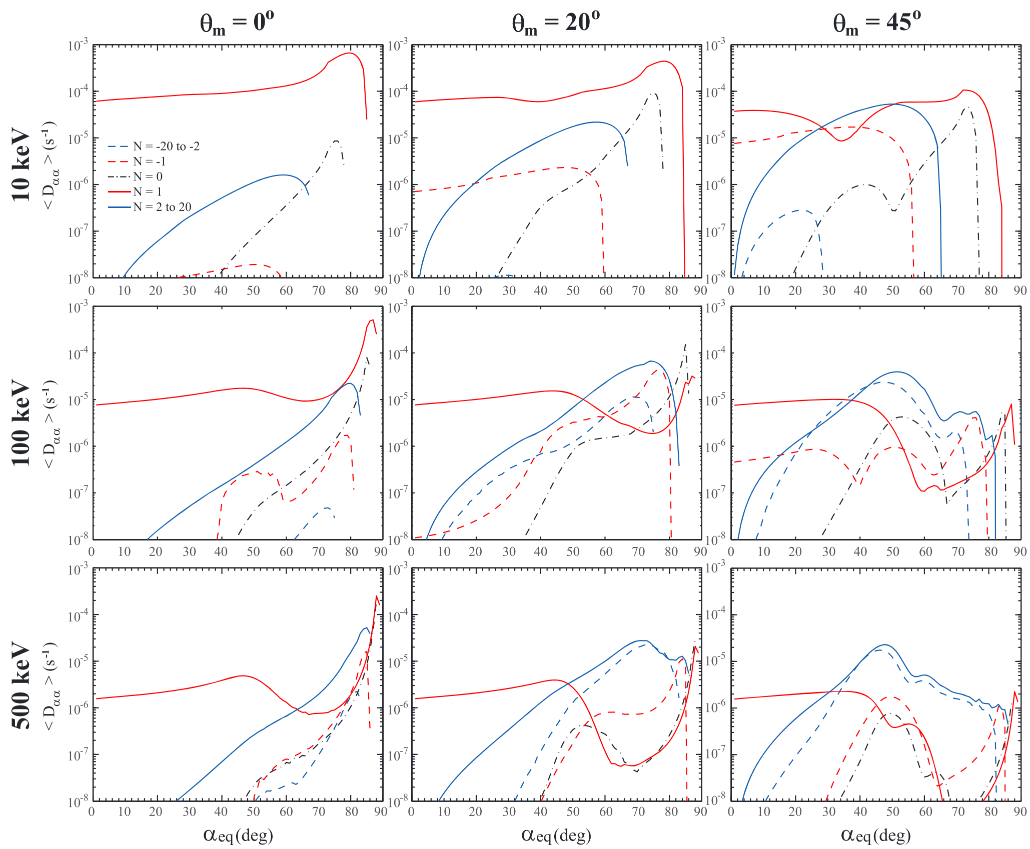

Figure 3. Bounce-averaged pitch angle diffusion coefficients of different resonance orders N as a function of proton equatorial pitch angle α_{eq} for different proton energies and peak wave normal angles θ_m, while the angular width $\theta_w = 5°$ remains constant.

found at $\alpha_{eq} > 70°$. For higher-energy protons, the pitch angle scattering at $\alpha_{eq} < 20°$ is almost unaffected by the variation of θ_m and θ_w, while the scattering rates at higher α_{eq} are strongly affected. As the waves become oblique, scattering rates of 100 and 500 keV protons increase at intermediate α_{eq} and decrease at high α_{eq} close to 90°, thus showing a strong dependence on both θ_m and θ_w. Pitch-angle coverage where the associated scattering rates increase becomes narrow and shifts to lower α_{eq} as θ_m or θ_w increases, and the reduction of scattering rates is mainly confined to $\alpha_{eq} > 80°$. Thus, the field-aligned propagation assumption for EMIC waves will break down for the resonant interactions with >10 keV protons, and results in a pronounced underestimate of the pitch angle scattering at intermediate pitch angles and overestimates the scattering of near-equatorially mirroring protons by orders of magnitude. Such changes in diffusion coefficients at high pitch angles for oblique EMIC waves can cause the change of the pitch angle distribution of protons but do not significantly affect their loss time scales, since the loss time scales are mainly controlled by the pitch angle scattering rate near the edge of the loss cone (Shprits, Li, et al., 2006). Nevertheless, for highly oblique EMIC waves, the deep minima in diffusion coefficients at high pitch angles not only affect the pitch angle evolution of >10 keV protons but also cause a pronounced increase of their loss time scale, according to Albert and Shprits (2008) and Shprits, Li, et al. (2006).

To understand the significant differences in scattering rates between different wave normal angle models, in Figure 3 we calculate the bounce-averaged pitch angle diffusion coefficients of 10, 100, and 500 keV protons for different resonance orders N corresponding to three indicated peak wave normal angles θ_m, while the angular width $\theta_w = 5°$ is kept constant. It is shown that the first-order resonance ($N = 1$) dominates the pitch angle scattering at low pitch angles and contributes to the diffusive transport of protons into the loss cone, while Landau resonance ($N = 0$) and high-order resonances ($|N| \geq 2$) mainly occur at larger pitch angles. An increase of θ_m will not obviously change the net diffusion coefficients of 10 keV protons, since the

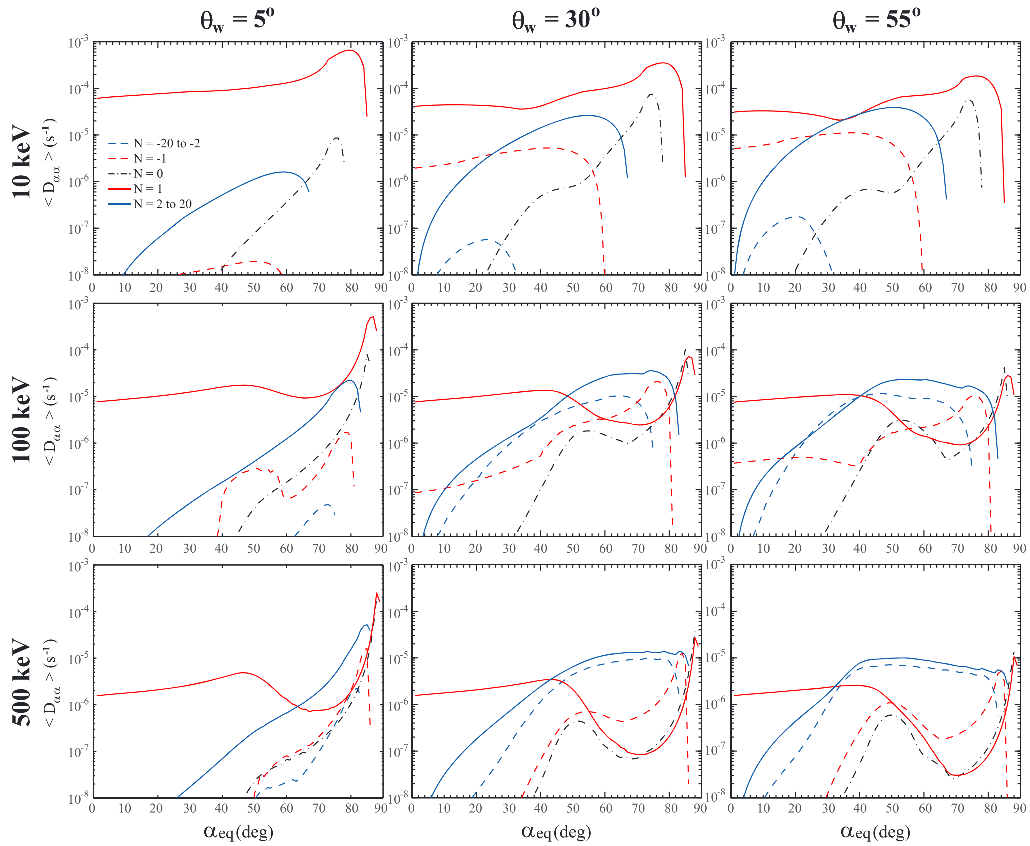

Figure 4. Same as in Figure 3, except for different angular widths θ_w and a fixed peak wave normal angle $\theta_m = 0°$.

reduction of scattering rates at α_{eq} = ~20°–50° for the first-order resonance will be compensated by the positive high-order resonances (i.e., $N \geq 2$). It is also shown that the scattering rates of higher-energy protons for the first-order resonance decrease deeply at $\alpha_{eq} > 50°$ as θ_m increases. Especially for $\theta_m = 45°$, the scattering rates at high pitch angles can be 2 orders lower than those for $\theta_m = 0°$. Furthermore, we find that both the increase of proton energy and θ_m can strongly increase the contributions of high-order resonances to the net scattering rates. For oblique waves, high-order resonances dominate the scattering at α_{eq} = ~40°–80° of 100 and 500 keV protons, which can account for the larger scattering rates at intermediate pitch angles as compared with field-aligned waves (as shown in Figure 2). However, the net contributions from high-order resonances cannot compensate for the decrease of first-order resonance scattering rates at $\alpha_{eq} > 80°$, which can help explain the much weaker scattering efficiency of >10 keV protons for $\alpha_{eq} > 80°$ presented in Figures 1 and 2.

Figure 4 shows how different order resonance scattering contributes to the net scattering rates for three indicated widths of the wave normal distribution ($\theta_w = 0°$, 30°, and 55°), while the peak normal angle $\theta_m = 0°$ remains constant. It is illustrated that the first-order resonance dominates at 10 keV for most pitch angles and dominates at all proton energies for low pitch angles. Similar to the results shown in Figure 3, a widening of the wave normal distribution will cause a stronger high-order scattering at higher energies, which can compensate for the significant decrease of first-order scattering at intermediate pitch angles. Even though the Landau resonance also contributes to the scattering of $\alpha_{eq} > 80°$ protons for a wide spectrum of wave normal angle, the combined scattering of $\alpha_{eq} > 80°$ protons by Landau resonance and first-order resonance is still much weaker than that for field-aligned waves.

4. Discussion and Conclusions

In the present study we investigate the sensitivity of EMIC wave-driven scattering loss of ring current protons to the wave normal angle distribution. We vary the peak normal angle and angular width to calculate the quasi-linear bounce-averaged pitch angle diffusion coefficients in a multiion (H^+, He^+, and O^+) plasma. The contributions of different resonance orders are also studied to understand the differences in the diffusion coefficients between field-aligned and obliquely propagating waves.

The principal conclusions of this study are as follows:

1. The wave normal distribution strongly affects the EMIC wave-driven scattering of ring current protons. Our results show that the discrepancies in the proton scattering rates between field-aligned and oblique waves become more pronounced with increases in the peak normal angle and angular width.
2. Pitch-angle scattering of higher-energy protons is more sensitive to the variation of wave normal distribution than that of lower energy protons. While the increase of θ_m or θ_w reduces the pitch angle scattering rates of ≤10 keV protons, the assumption of field-aligned propagation can cause a pronounced underestimate of the pitch angle scattering of intermediate equatorial pitch angle protons and an overestimate the scattering of high equatorial pitch angle protons above 10 keV. Especially for highly oblique waves, scattering rates for near-equatorially mirroring protons can be 2 orders of magnitude lower than those for field-aligned waves.
3. The first-order resonance dominates the pitch angle scattering at low pitch angles, regardless of the wave normal distribution. As the increase of peak normal angle or angular width, the scattering rates of >10 keV protons due to the first-order resonance decrease sharply for equatorial pitch angles $\alpha_{\text{eq}} > 50°$. However, the contributions of high-order resonances to the net scattering rates become important for oblique waves and can compensate for the significant decrease of first-order resonant scattering rates at intermediate pitch angles. This can explain the higher net scattering rates of >10 keV protons at intermediate pitch angles as compared with those for field-aligned waves.

Our results show that knowledge of the wave normal distribution of EMIC waves is essential for evaluating the pitch angle diffusion coefficients of ring current protons due to EMIC waves. The field-aligned propagation approximation, which has been widely used in previous studies, can break down for the resonant interactions between EMIC waves and ring current protons. We suggest that the variation of wave normal distribution not only affects the pitch angle evolution of ring current protons but also results in the change of their loss time scale. Especially for highly oblique EMIC waves, the much weaker scattering efficiency of >10 keV protons near 90° pitch angles than that of lower pitch angles may lead to a “top-hat” pitch angle distribution of protons. Therefore, it is necessary to conduct a realistic treatment of the EMIC wave normal distribution, such as the development of a global empirical model that can take into account the dependence of EMIC wave normal angle on L-shell, magnetic local time, and geomagnetic latitude. Future modeling efforts are required to incorporate reliable EMIC wave normal angle distributions for improved understanding of the pitch angle evolution and scattering loss of ring current protons.

Acknowledgments
The work was supported by the NSFC grants 41674163, 41474141, and 41204120 and the Hubei Province Natural Science Excellent Youth Foundation (2016CFA044). D.S. acknowledges support from a Discovery Grant of the Natural Sciences and Engineering Research Council of Canada. No data sets were used for this study. The numerical results can be obtained from https://dx.doi.org/10.6084/m9.figshare.7410440.

References

Albert, J. M. (2003). Evaluation of quasi-linear diffusion coefficients for EMIC waves in a multispecies plasma. *Journal of Geophysical Research*, *108*(A6), 1249. https://doi.org/10.1029/2002JA009792

Albert, J. M. (2007). Simple approximations of quasi-linear diffusion coefficients. *Journal of Geophysical Research*, *112*, A12202. https://doi.org/10.1029/2007JA012551

Albert, J. M. (2017). Quasi-linear diffusion coefficients for highly oblique whistler mode waves. *Journal of Geophysical Research: Space Physics*, *122*, 5339–5354. https://doi.org/10.1002/2017JA024124

Albert, J. M., & Shprits, Y. Y. (2008). Estimates of lifetimes against pitch angle diffusion. *Journal of Atmospheric and Solar - Terrestrial Physics*, *71*(16), 1647–1652. https://doi.org/10.1016/j.jastp.2008.07.004

Allen, R. C., Zhang, J. C., Kistler, L. M., Spence, H. E., Lin, R. L., Klecker, B., et al. (2015). A statistical study of EMIC waves observed by Cluster: 1. Wave properties. *Journal of Geophysical Research: Space Physics*, *120*, 5574–5592. https://doi.org/10.1002/2015JA021333

Anderson, B. J., Denton, R. E., Ho, G., Hamilton, D. C., Fuselier, S. A., & Strangeway, R. J. (1996). Observational test of local proton cyclotron instability in the Earth's magnetosphere. *Journal of Geophysical Research*, *101*, 21,527–21,543. https://doi.org/10.1029/96JA01251

Artemyev, A., Agapitov, O., Breuillard, H., Krasnoselskikh, V., & Rolland, G. (2012). Electron pitch-angle diffusion in radiation belts: The effects of whistler wave oblique propagation. *Geophysical Research Letters*, *39*, L08105. https://doi.org/10.1029/2012GL051393

Cao, X., Ni, B., Liang, J., Xiang, Z., Wang, Q., Shi, R., et al. (2016). Resonant scattering of central plasma sheet protons by multiband EMIC waves and resultant proton loss timescales. *Journal of Geophysical Research: Space Physics*, *121*, 1219–1232. https://doi.org/10.1002/2015JA021933

Cao, X., Ni, B., Summers, D., Bortnik, J., Tao, X., Shprits, Y. Y., et al. (2017). Bounce resonance scattering of radiation belt electrons by H^+ band EMIC waves. *Journal of Geophysical Research: Space Physics*, *122*, 1702–1713. https://doi.org/10.1002/2016JA023607

Cao, X., Shprits, Y. Y., Ni, B., & Zhelavskaya, I. S. (2017). Scattering of ultra-relativistic electrons in the Van Allen radiation belts accounting for hot plasma effects. *Scientific Reports*, *7*(1), 17719. https://doi.org/10.1038/s41598-017-17739-7

Chen, L., Thorne, R. M., Jordanova, V. K., Wang, C.-P., Gkioulidou, M., Lyons, L., & Horne, R. B. (2010). Global simulation of EMIC wave excitation during the 21 April 2001 storm from coupled RCM-RAM-HOTRAY modeling. *Journal of Geophysical Research*, *115*, A07209. https://doi.org/10.1029/2009JA015075

Cornwall, J. M. (1965). Cyclotron instabilities and electromagnetic emission in the ultra low frequency and very low frequency ranges. *Journal of Geophysical Research*, *70*, 61–69. https://doi.org/10.1029/JZ070i001p00061

Daglis, I. A., Thorne, R. M., Baumjohann, W., & Orsini, S. (1999). The terrestrial ring current: Origin, formation, and decay. *Reviews of Geophysics*, *37*, 407–438. https://doi.org/10.1029/1999RG900009

Erlandson, R. E., & Ukhorskiy, A. J. (2001). Observations of electromagnetic ion cyclotron waves during geomagnetic storms: Wave occurrence and pitch angle scattering. *Journal of Geophysical Research*, *106*, 3883–3895. https://doi.org/10.1029/2000JA000083

Fuselier, S. A., Gary, S. P., Thomsen, M. F., Claflin, E. S., Hubert, B., Sandel, B. R., & Immel, T. (2004). Generation of transient dayside subauroral proton precipitation. *Journal of Geophysical Research*, *109*, A12227. https://doi.org/10.1029/2004JA010393

Gamayunov, K. V., Khazanov, G. V., Liemohn, M. W., Fok, M.-C., & Ridley, A. J. (2009). Self-consistent model of magnetospheric electric field, ring current, plasmasphere, and electromagnetic ion cyclotron waves: Initial results. *Journal of Geophysical Research*, *114*, A03221. https://doi.org/10.1029/2008JA013597

Gao, Y., Xiao, F., Yan, Q., Yang, C., Liu, S., He, Y., & Zhou, Q. (2015). Influence of wave normal angles on hiss-electron interaction in Earth's slot region. *Journal of Geophysical Research: Space Physics*, *120*, 9385–9400. https://doi.org/10.1002/2015JA021786

Gkioulidou, M., Ukhorskiy, A. Y., Mitchell, D. G., & Lanzerotti, L. J. (2016). Storm time dynamics of ring current protons: Implications for the long-term energy budget in the inner magnetosphere. *Geophysical Research Letters*, *43*, 4736–4744. https://doi.org/10.1002/2016GL068013

Glauert, S. A., & Horne, R. B. (2005). Calculation of pitch angle and energy diffusion coefficients with the PADIE code. *Journal of Geophysical Research*, *110*, A04206. https://doi.org/10.1029/2004JA010851

He, F., Cao, X., Ni, B., Xiang, Z., Zhou, C., Gu, X., et al. (2016). Combined scattering loss of radiation belt relativistic electrons by simultaneous three-band EMIC waves: A case study. *Journal of Geophysical Research: Space Physics*, *121*, 4446–4451. https://doi.org/10.1002/2016JA022483

Jordanova, V. K., Farrugia, C. J., Thorne, R. M., Khazanov, G. V., Reeves, G. D., & Thomsen, M. F. (2001). Modeling ring current proton precipitation by electromagnetic ion cyclotron waves during the May 14–16, 1997, storm. *Journal of Geophysical Research*, *106*, 7–22. https://doi.org/10.1029/2000JA002008

Jordanova, V. K., Kozyra, J. U., Nagy, A. F., & Khazanov, G. V. (1997). Kinetic model of the ring current-atmosphere interactions. *Journal of Geophysical Research*, *102*, 14,279–14,291. https://doi.org/10.1029/96JA03699

Kersten, T., Horne, R. B., Glauert, S. A., Meredith, N. P., Fraser, B. J., & Grew, R. S. (2014). Electron losses from the radiation belts caused by EMIC waves. *Journal of Geophysical Research: Space Physics*, *119*, 8820–8837. https://doi.org/10.1002/2014JA020366

Khazanov, G. V., Gamayunov, K. V., Gallagher, D. L., & Kozyra, J. U. (2006). Self-consistent model of magnetospheric ring current and propagating electromagnetic ion cyclotron waves: Waves in multi-ion magnetosphere. *Journal of Geophysical Research*, *111*, A10202. https://doi.org/10.1029/2006JA011833

Kozyra, J. U., Jordanova, V. K., Home, R. B., & Thorne, R. M. (2013). Modeling of the contribution of electromagnetic ion cyclotron (EMIC) waves to stormtime ring current erosion. In B. T. Tsurutani, W. D. Gonzalez, Y. Kamide, & J. K. Arballo (Eds.), *Magnetic Storms*, *Geophys. Monogr. Ser.* (Vol. 98, pp. 187–202). Washington, DC: AGU. https://doi.org/10.1029/GM098p0187

Lei, M., Xie, L., Li, J., Pu, Z., Fu, S., Ni, B., et al. (2017). The radiation belt electron scattering by magnetosonic wave: Dependence on key parameters. *Journal of Geophysical Research: Space Physics*, *122*, 12,338–12,352. https://doi.org/10.1002/2016JA023801

Li, W., Mourenas, D., Artemyev, A. V., Agapitov, O. V., Bortnik, J., Albert, J. M., et al. (2014). Evidence of stronger pitch angle scattering loss caused by oblique whistler-mode waves as compared with quasi-parallel waves. *Geophysical Research Letters*, *41*, 6063–6070. https://doi.org/10.1002/2014GL061260

Li, W., Shprits, Y. Y., & Thorne, R. M. (2007). Dynamic evolution of energetic outer zone electrons due to wave-particle interactions during storms. *Journal of Geophysical Research*, *112*, A10220. https://doi.org/10.1029/2007JA012368

Liang, J., Donovan, E., Ni, B., Yue, C., Jiang, F., & Angelopoulos, V. (2014). On an energy-latitude dispersion pattern of ion precipitation potentially associated with magnetospheric EMIC waves. *Journal of Geophysical Research: Space Physics*, *119*, 8137–8160. https://doi.org/10.1002/2014JA020226

Liu, K., Lemons, D. S., Winske, D., & Gary, S. P. (2010). Relativistic electron scattering by electromagnetic ion cyclotron fluctuations: Test particle simulations. *Journal of Geophysical Research*, *115*, A04204. https://doi.org/10.1029/2009JA014807

Meredith, N. P., Horne, R. B., Glauert, S. A., & Anderson, R. R. (2007). Slot region electron loss timescales due to plasmaspheric hiss and lightning-generated whistlers. *Journal of Geophysical Research*, *112*, A08214. https://doi.org/10.1029/2007JA012413

Meredith, N. P., Thorne, R. M., Horne, R. B., Summers, D., Fraser, B. J., & Anderson, R. R. (2003). Statistical analysis of relativistic electron energies for cyclotron resonance with EMIC waves observed on CRRES. *Journal of Geophysical Research*, *108*(A6), 1250. https://doi.org/10.1029/2002JA009700

Min, K., Lee, J., Keika, K., & Li, W. (2012). Global distribution of EMIC waves derived from THEMIS observations. *Journal of Geophysical Research*, *117*, A05219. https://doi.org/10.1029/2012JA017515

Miyoshi, Y., Sakaguchi, K., Shiokawa, K., Evans, D., Albert, J., Connors, M., & Jordanova, V. (2008). Precipitation of radiation belt electrons by EMIC waves, observed from ground and space. *Geophysical Research Letters*, *35*, L23101. https://doi.org/10.1029/2008GL035727

Mourenas, D., Artemyev, A. V., Ripoll, J.-F., Agapitov, O. V., & Krasnoselskikh, V. V. (2012). Timescales for electron quasi-linear diffusion by parallel and oblique lower-band chorus waves. *Journal of Geophysical Research*, *117*, A06234. https://doi.org/10.1029/2012JA017717

Ni, B., Cao, X., Shprits, Y. Y., Summers, D., Gu, X., Fu, S., & Lou, Y. (2018). Hot plasma effects on the cyclotron-resonant pitch-angle scattering rates of radiation belt electrons due to EMIC waves. *Geophysical Research Letters*, *45*, 21–30. https://doi.org/10.1002/2017GL076028

Ni, B., Cao, X., Zou, Z., Zhou, C., Gu, X., Bortnik, J., et al. (2015). Resonant scattering of outer zone relativistic electrons by multiband EMIC waves and resultant electron loss time scales. *Journal of Geophysical Research: Space Physics*, *120*, 7357–7373. https://doi.org/10.1002/2015JA021466

Ni, B., Thorne, R. M., Shprits, Y. Y., & Bortnik, J. (2008). Resonant scattering of plasma sheet electrons by whistler-mode chorus: Contribution to diffuse auroral precipitation. *Geophysical Research Letters*, *35*, L11106. https://doi.org/10.1029/2008GL034032

Rodger, C. J., Raita, T., Clilverd, M. A., Seppälä, A., Dietrich, S., Thomson, N. R., & Ulich, T. (2008). Observations of relativistic electron precipitation from the radiation belts driven by EMIC waves. *Geophysical Research Letters*, *35*, L16106. https://doi.org/10.1029/2008GL034804

Runov, A., Zhang, X. J., & Angelopoulos, V. (2016). Evolution of partial ring current ion pitch angle distributions during the main phase of a storm on 17 March 2015. *Journal of Geophysical Research: Space Physics*, *121*, 5284–5293. https://doi.org/10.1002/2016JA022391

Saikin, A. A., Zhang, J.-C., Allen, R. C., Smith, C. W., Kistler, L. M., Spence, H. E., et al. (2015). The occurrence and wave properties of H^+-, He^+-, and O^+-band EMIC waves observed by the Van Allen probes. *Journal of Geophysical Research: Space Physics*, *120*, 7477–7492. https://doi.org/10.1002/2015JA021358

Sakaguchi, K., Shiokawa, K., Ieda, A., Miyoshi, Y., Otsuka, Y., Ogawa, T., et al. (2007). Simultaneous ground and satellite observations of an isolated proton arc at subauroral latitudes. *Journal of Geophysical Research*, *112*, A04202. https://doi.org/10.1029/2006JA012135

Sheeley, B. W., Moldwin, M. B., Rassoul, H. K., & Anderson, R. R. (2001). An empirical plasmasphere and trough density model: CRRES observations. *Journal of Geophysical Research*, *106*, 25,631–25,641. https://doi.org/10.1029/2000JA000286

Shprits, Y. Y., Drozdov, A. Y., Spasojevic, M., Kellerman, A. C., Usanova, M. E., Engebretson, M. J., et al. (2016). Wave-induced loss of ultra-relativistic electrons in the Van Allen radiation belts. *Nature Comms.*, *7*(1), 12883. https://doi.org/10.1038/ncomms12883

Shprits, Y. Y., Kellerman, A., Aseev, N., Drozdov, A. Y., & Michaelis, I. (2017). Multi-MeV electron loss in the heart of the radiation belts. *Geophysical Research Letters*, *44*, 1204–1209. https://doi.org/10.1002/2016GL072258

Shprits, Y. Y., Li, W., & Thorne, R. M. (2006). Controlling effect of the pitch angle scattering rates near the edge of the loss cone on electron lifetimes. *Journal of Geophysical Research*, *111*, A12206. https://doi.org/10.1029/2006JA011758

Shprits, Y. Y., & Ni, B. (2009). Dependence of the quasi-linear scattering rates on the wave normal distribution of chorus waves. *Journal of Geophysical Research*, *114*, A11205. https://doi.org/10.1029/2009JA014223

Shprits, Y. Y., Thorne, R. M., Horne, R. B., & Summers, D. (2006). Bounce-averaged diffusion coefficients for field-aligned chorus waves. *Journal of Geophysical Research*, *111*, A10225. https://doi.org/10.1029/2006JA011725

Spasojevic, M., Blum, L. W., MacDonald, E. A., Fuselier, S. A., & Golden, D. I. (2011). Correspondence between a plasma-based EMIC wave proxy and subauroral proton precipitation. *Geophysical Research Letters*, *38*, L23102. https://doi.org/10.1029/2011GL049735

Su, Z., Zong, Q.-G., Yue, C., Wang, Y., Zhang, H., & Zheng, H. (2011). Proton aurorual intensification induced by interplanetary shock on 7 November 2004. *Journal of Geophysical Research*, *116*, A08223. https://doi.org/10.1029/2010JA016239

Summers, D. (2005). Quasi-linear diffusion coefficients for field-aligned electromagnetic waves with applications to the magnetosphere. *Journal of Geophysical Research*, *110*, A08213. https://doi.org/10.1029/2005JA011159

Summers, D., Ni, B., & Meredith, N. P. (2007a). Timescales for radiation belt electron acceleration and loss due to resonant wave-particle interactions: 2. Evaluation for VLF chorus, ELF hiss, and electromagnetic ion cyclotron waves. *Journal of Geophysical Research*, *112*, A04207. https://doi.org/10.1029/2006JA011993

Summers, D., Ni, B., & Meredith, N. P. (2007b). Timescales for radiation belt electron acceleration and loss due to resonant wave-particle interactions: 1. Theory. *Journal of Geophysical Research*, *112*, A04206. https://doi.org/10.1029/2006JA011801

Summers, D., & Thorne, R. M. (2003). Relativistic electron pitch angle scattering by electromagnetic ion cyclotron waves during geomagnetic storms. *Journal of Geophysical Research*, *108*(A4), 1143. https://doi.org/10.1029/2002JA009489

Usanova, M. E., Drozdov, A., Orlova, K., Mann, I. R., Shprits, Y., Robertson, M. T., et al. (2014). Effect of EMIC waves on relativistic and ultrarelativistic electron populations: Ground-based and Van Allen Probes observations. *Geophysical Research Letters*, *41*, 1375–1381. https://doi.org/10.1002/2013GL059024

Usanova, M. E., Mann, I. R., Kale, Z. C., Rae, I. J., Sydora, R. D., Sandanger, M., et al. (2010). Conjugate ground and multisatellite observations of compression-related EMIC Pc1 waves and associated proton precipitation. *Journal of Geophysical Research*, *115*, A07208. https://doi.org/10.1029/2009JA014935

Wang, Q., Cao, X., Gu, X., Ni, B., Zhou, C., Shi, R., & Zhao, Z. (2016). A parametric study of the linear growth of magnetospheric EMIC waves in a hot plasma. *Physics of Plasmas*, *23*(6), 062903. https://doi.org/10.1063/1.4953565

Xiao, F., Chen, L., He, Y., Su, Z., & Zheng, H. (2011). Modeling of precipitation loss of ring current protons by electromagnetic ion cyclotron waves. *Journal of Atmospheric and Solar - Terrestrial Physics*, *73*, 106–111. https://doi.org/10.1016/j.jastp.2010.01.007

Xiao, F., Yang, C., Zhou, Q., He, Z., He, Y., Zhou, X., & Tang, L. (2012). Nonstorm time scattering of ring current protons by electromagnetic ion cyclotron waves. *Journal of Geophysical Research*, *117*, A08204. https://doi.org/10.1029/2012JA017922

Xiao, F., Zong, Q., Su, Z., Yang, C., He, Z., Wang, Y., & Gao, Z. (2013). Determining the mechanism of cusp proton aurora. *Scientific Reports*, *3*(1), 1–15. https://doi.org/10.1038/srep01654

Yahnin, A., & Yahnina, T. (2007). Energetic proton precipitation related to ion-cyclotron waves. *Journal of Atmospheric and Solar - Terrestrial Physics*, *69*(14), 1690–1706. https://doi.org/10.1016/j.jastp.2007.02.010

Zhang, J.-C., Saikin, A. A., Kistler, L. M., Smith, C. W., Spence, H. E., Mouikis, C. G., et al. (2014). Excitation of EMIC waves detected by the Van Allen probes on 28 April 2013. *Geophysical Research Letters*, *41*, 4101–4108. https://doi.org/10.1002/2014GL060621

Zhang, X.-J., Li, W., Ma, Q., Thorne, R. M., Angelopoulos, V., Bortnik, J., et al. (2016). Direct evidence for EMIC wave scattering of relativistic electrons in space. *Journal of Geophysical Research: Space Physics*, *121*, 6620–6631. https://doi.org/10.1002/2016JA022521

Zhao, H., Li, X., Baker, D. N., Fennell, J. F., Blake, J. B., Larsen, B. A., et al. (2015). The evolution of ring current ion energy density and energy content during geomagnetic storms based on Van Allen Probes measurements. *Journal of Geophysical Research: Space Physics*, *120*, 7493–7511. https://doi.org/10.1002/2015JA021533